Chapter 1

BKT physics with two-dimensional atomic gases

Zoran Hadzibabic[(1)] and Jean Dalibard[(2)]

[(1)] *Cavendish Laboratory, University of Cambridge*
JJ Thomson Avenue, Cambridge CB3 0HE, United Kingdom
[(2)] *Laboratoire Kastler Brossel, CNRS, UPMC, École normale supérieure*
24 rue Lhomond, 75005 Paris, France

In this chapter we review the recent advances in experimental investigation and theoretical understanding of Berezinskii–Kosterlitz–Thouless (BKT) physics in ultracold trapped atomic gases. We explain how to produce quasi two-dimensional (2D) samples by freezing out one degree of freedom with laser beams, and we detail the modelling of atomic interactions in this constrained geometry. We discuss some remarkable properties of the equation of state of dilute 2D Bose gases, such as its scale invariance. We also comment on the "competition" between the superfluid, BKT-driven phase transition in a homogenous 2D fluid of bosons, and the more conventional Bose–Einstein condensation that is expected for an ideal 2D Bose gas confined in a harmonic potential. We present some experimental techniques that allow one to measure the equation of state of the gas, monitor the occurrence of a BKT-driven phase transition, and observe thermally activated quantized vortices, which constitute the microscopic building block of the BKT mechanism.

1.1. Introduction

In recent years ultracold atomic gases have emerged as a versatile playground for studies of fundamental many-body physics.[1–5] The appeal of these systems stems from a high degree of control available to the experimentalists in designing their properties such as the strength of inter-atomic interactions or the geometry of the external potential the atoms live in. In this respect, some of the most exciting developments have been associated with the possibility to trap and study quantum degenerate atomic samples in reduced dimensionality.[3]

The physics explored with atomic gases is believed to be universal in the sense that fundamentally analogous phenomena occur in a range of more "conventional" condensed-matter systems, such as liquid helium and solid state materials. At the same time, the experimental methods in atomic physics, and in particular the probes of many-body behaviour, are quite different from those used in the traditional condensed matter research. This often offers a complementary view on some long-

studied problems.

Here we will give an overview of the progress in theoretical understanding and experimental investigation of the Berezinskii–Kosterlitz–Thouless[6,7] (BKT) physics occurring in atomic Bose gases confined to two spatial dimensions (2D). In this context, these systems are conceptually closest to ^{4}He films, in which BKT superfluid phenomena have first been observed more than 30 years ago.[8] In order to highlight the new insights into the physics of 2D Bose fluids, whether already experimentally demonstrated or still just theoretically anticipated, we will in particular focus on the differences between atomic gases and liquid helium films. These are primarily associated with three experimental aspects of ultracold atom research:

(1) In contrast to the spatially uniform helium films, ultracold atomic gases are produced in harmonic (in-plane) trapping potentials.

(2) The inter-particle interactions in a dilute atomic gas are usually significantly weaker than in liquid helium. Moreover the strength of interactions varies between different experimental setups, and can in principle even be continuously tuned in a single experiment, using so-called Fano–Feshbach resonances.[9]

(3) The experimental probes of atomic physics, in particular matter-wave interferometry, can give direct access to the coherence (phase) properties of a 2D gas.

Before discussing the physics of 2D Bose gases in greater detail in the following sections, we briefly anticipate some salient points:

The importance of the in-plane harmonic trapping potential is clear from the very general point of view of the properties of phase transitions in 2D systems. Historically, the BKT theory was necessary to explain how a phase transition to a superfluid state can occur in a 2D Bose fluid at a non-zero temperature T, despite the fact that the Mermin–Wagner theorem[10,11] forbids emergence of a true long range order (LRO) associated with Bose–Einstein condensation (BEC). The destruction of true LRO at any non-zero T is a consequence of the functional form of the density of states for the long-wavelength, low-energy excitations in a uniform 2D system. In a 2D harmonic trap this functional form is different, and at first sight the Mermin–Wagner conclusion no longer holds. Specifically, for an ideal (non-interacting) harmonically-trapped 2D Bose gas one can easily show that the standard Einstein's statistical argument predicts the existence of a BEC transition at a non-zero critical temperature. One could therefore jump to the conclusion that the case of a 2D Bose gas in a harmonic trap is "trivial", since conventional LRO is possible and one does not need to invoke the more subtle BKT theory to understand this system.

This is however not the case. A more detailed analysis reveals that the case of an ideal atomic gas is anomalous; in any real (interacting) system the conventional BEC transition is suppressed and replaced by the BKT one. We can now anticipate the two-fold importance of the possibility to experimentally tune the strength of interactions in an atomic gas. First, quite generally, the BKT transition in a Bose

fluid is fundamentally mediated by interactions and many of its properties (such as the critical temperature) crucially depend on their strength. Second, specifically in the case of a harmonically trapped gas, the fact that in the limit of vanishing interactions we should recover the conventional BEC transition remains true. This, together with the finite size effects which are ubiquitous in all experimental 2D systems, leads to a interesting interplay between BKT and BEC physics.

Finally, the ability to experimentally probe the coherence properties of atomic gases makes studies of BKT physics in these systems quite complementary to the traditional experiments on helium films. From a theoretical point of view, the microscopic description of a Bose fluid at low (but non-zero) temperature is largely related to the phase properties of the macroscopic wavefunction describing the system. At sufficiently low T the density fluctuations in the fluid are strongly suppressed and the low-energy thermal fluctuations which destroy the LRO are almost purely phase excitations. The transition from the superfluid to the normal state is driven by the proliferation of single quantized vortices, which are topological phase defects. The absence of LRO on both sides of the BKT critical point (in the thermodynamic limit of an infinite system) is seen in the fact that the first-order correlation function $g_1(\boldsymbol{r})$ vanishes for $r \to \infty$, and the distinction between the superfluid and the normal state is seen in the functional form of the decay of g_1 with distance r. From an experimental point of view the emergence of a non-zero superfluid fraction below a critical temperature constitutes the macroscopic signature of BKT physics, and it has been studied with great success in transport experiments with liquid helium. Atomic gases on the other hand offer the potential for a more direct access to the underlying microscopic physics. Specifically, matter-wave interference experiments allow both a direct visualisation of the vortices which drive the BKT transition, and measurements of the off-diagonal correlation function g_1.

1.2. Experimental realizations

We start our discussion of the physics of atomic 2D Bose gases with a brief description of the setups that allow one to produce fluids with an effective reduced dimensionality. In order to realise such systems, one uses a strongly anisotropic trap so the particle motion is very tightly confined along one direction, say z, and more loosely confined in the orthogonal plane. In practice the potential along z can be treated as harmonic, $U(z) = m\omega_z^2 z^2/2$, where m is the atomic mass. The oscillation frequency ω_z is chosen such that $\hbar\omega_z$ is significantly larger than the thermal energy $k_{\rm B}T$ and the interaction energy between particles. The atoms thus occupy essentially the ground state of the z motion, which has the extension $a_z = (\hbar/m\omega_z)^{1/2}$. Here we briefly review the various techniques to produce the required $U(z)$, we give the typical values of the parameters of the gas, and we explain how one can describe interactions between atoms for this trapping geometry.

1.2.1. *Freezing-out one spatial degree of freedom*

The dipole potential. In order to confine atomic motion in the z direction, one generally uses a spatially varying *dipole potential* which appears when an atom is placed in a monochromatic laser beam with an intensity gradient.[12] Within the electric dipole approximation, the strength of the atom-light coupling is characterized by the Rabi frequency $\kappa(\boldsymbol{r}) = d\,E(\boldsymbol{r})/\hbar$, where d is the atomic dipole and $E(\boldsymbol{r})$ the modulus of the local electric field. When the detuning Δ between the laser frequency and the atomic resonance frequency is chosen much larger than κ, the dipole potential reads $U = \hbar\kappa^2/4\Delta$, and corresponds to the light shift (or ac-Stark shift) of the atomic ground state. When the laser is blue-detuned ($\Delta > 0$) [resp. red-detuned ($\Delta < 0$)] with respect to the atomic resonance, the atoms are attracted towards the low-intensity [resp. high-intensity] regions. Typical depths of optical traps range from 1 μK to several tens of mK, depending on the available laser power, the size of the beams and the choice of detuning. The choice of these parameters generally results from a trade-off between the need for a large depth, which is obtained for small detunings, and the reduction of heating due to random scattering of laser photons, whose rate scales as Δ^{-2} and which thus favours large detunings. Note that other confinement schemes, such as magnetic traps and dressing of atoms with radio-frequency waves, have also been investigated to freeze the motion of the atoms along one direction.[13]

A single atomic plane. Conceptually the simplest laser configuration that provides the required confinement along z consists in a single light beam that is prepared in a TEM_{00} Gaussian mode and that propagates along x. Using cylindrical lenses, one produces a tight focus along the z direction and a much looser focus along y. The light is red-detuned with respect to the atomic resonance and the atoms accumulate around the focal point of the beam.[14,15] This simple scheme works well in practice, but it suffers from a lack of flexibility: one cannot control independently the confinement along the z axis and the confinement in the xy plane, since the laser beam affects all three motions. A more versatile setup consists in a blue-detuned laser beam prepared in a Hermite–Gauss mode, also propagating along x, with a node in the $z = 0$ plane.[16,17] The confinement in the xy plane is then provided by different means, either another laser beam or a magnetic trap.

Parallel atomic layers. For some applications it is useful to prepare simultaneously several parallel planes of atoms. This can be achieved using a 1D optical lattice, *i.e.* a laser standing wave along the z-axis.[18–22] Depending on the sign of Δ, the atoms accumulate at the nodes or the antinodes of the standing wave. In order to control the distance between planes, one can produce the standing wave with two beams crossing at an angle smaller than 180 degrees.[23–26] By changing the intensity and the spatial period of the optical lattice, one can adjust the number of significantly populated planes from one to several, and switch from a situation

where neighbouring layers are strongly coupled by quantum tunnelling, to the case where they can be considered as independent on the time scale of the experiment.

1.2.2. *Experimental procedure and parameters*

The production of a 2D gas usually starts with the realisation of a 3D bosonic or fermionic gas in the degenerate regime. The potential $U(z)$ producing the strong confinement of the z direction is then ramped up, and one is left with one (or several) flat gas(es). The oscillation frequency $\omega_z/2\pi$ along the strongly confined direction is in the 1-10 kHz range and the extension a_z along z is typically between 100 and 500 nm. The number of atoms in the 2D gas varies from a few thousands to 10^5. The temperature, ranging from 10 to a few hundred nanokelvins, is determined by the initial conditions of the 3D sample and an optional evaporative cooling in the 2D trap. For typical confinement in the xy directions, the size of the gas is equal to a few tens of micrometers. In most experiments so far the confinement in the xy plane is also harmonic, with frequencies ω_{xy} which are smaller than ω_z by one to three orders of magnitude. However one can also produce a "hard wall" type confinement, using an annulus of light propagating along the z axis.[27]

1.2.3. *Interactions*

Repulsive interactions between atoms play a central role in BKT physics. They are responsible for a strong reduction of density fluctuations in the normal phase. The atomic gas thus forms a medium that is essentially characterised by its phase fluctuations, and that can be directly mapped to the general problem discussed in the seminal BKT papers.[6,7]

The interaction strength $\tilde{g}$. Given the short-range nature of Van der Waals interactions between neutral atoms, one can treat them in first approximation by a contact potential and write the interaction energy in the 2D gas as[28]

$$E_{\rm int} = \frac{g}{2}\int \langle n^2(\boldsymbol{r})\rangle \, d^2r \quad \text{with} \quad g = \frac{\hbar^2}{m}\tilde{g}, \tag{1.1}$$

where $\tilde{g}$ is a dimensionless, constant coefficient characterising the strength of interactions. A value of $\tilde{g} \ll 1$ corresponds to a weakly interacting gas. The strongly interacting case, which is met for example with liquid helium films, is reached when $\tilde{g} \geq 1$. In order to evaluate $\tilde{g}$, one can start from the analogue of Eq. (1.1) for the three-dimensional case[1]

$$E_{\rm int} = \frac{2\pi\hbar^2 a_{\rm s}}{m}\int \langle n_3^2(\boldsymbol{r})\rangle \, d^3r, \tag{1.2}$$

where $a_{\rm s}$ is the scattering length and n_3 the 3D spatial density. We now use the ansatz $n_3(x,y,z) = n(x,y)\exp(-z^2/a_z^2)/\sqrt{\pi a_z^2}$, corresponding to the intuitive idea

that the motion along z is frozen to the ground state of the harmonic oscillator with frequency ω_z. We then find the value of $\tilde{g}$:

$$\tilde{g} = \sqrt{8\pi}\, a_{\rm s}/a_z. \tag{1.3}$$

The description of interactions in terms of the single constant parameter $\tilde{g}$ is usually sufficient for addressing the physics of cold atomic gases. However this description cannot be made fully consistent, as it is based on the notion of a contact interaction potential. Strictly speaking this potential is ill-defined in two dimensions because it leads to an ultra-violet divergence for the quantum two-body problem.[29] A more accurate way to evaluate the interaction energy consists in starting from the description of a binary collision between two atoms, with initial and final states whose z-dependence coincides with the ground state of the potential $U(z)$. The scattering amplitude $f(k)$ can then be written[28,30]

$$\frac{1}{f(k)} \approx \frac{1}{\tilde{g}} - \frac{1}{2\pi}\ln(ka_z) + \frac{i}{4}, \tag{1.4}$$

where $\tilde{g}$ is still given by (1.3). The expression (1.1) for the interaction energy assumes that $f(k)$ is energy-independent and $\approx \tilde{g}$, which is legitimate when $\tilde{g} \ll 1$.

The healing length. The length scale associated with the interaction energy gn is the *healing length* $\xi = 1/\sqrt{\tilde{g}n}$. It gives the characteristic size over which the density is significantly depleted around a point where n vanishes. In particular ξ can be viewed as the typical size for a vortex core. The number of 'missing atoms' due to the presence of a vortex is thus given by $\delta N \approx \pi\xi^2 n = \pi/\tilde{g}$. In the weakly interacting regime, $\tilde{g} \ll 1$ hence $\delta N \gg 1$, and a vortex corresponds to a significant density dip in the spatial distribution. In a strongly interacting gas $\delta N \sim 1$, which means that a vortex is an atomic-size defect in this case, with no detectable dip in the density profile of the fluid.

Fano–Feshbach resonances. A remarkable feature of cold atom physics is the possibility to control the interaction strength (*i.e.* the scattering length $a_{\rm s}$) using a scattering resonance, also called a Fano–Feshbach resonance.[9] To reach the resonance, one tunes the ambient magnetic field B in order to vary the energy of the ingoing channel of two colliding atoms with respect to another (closed) channel. The resonance occurs for a particular value B_0 of the ambient field, such that the asymptotic energy of the ingoing channel coincides with a bound state of the closed channel. Close to the resonance, the phase shift accumulated by the atom pair during the collision varies rapidly with B. The scattering length diverges at the resonance point $B = B_0$ and scales as $(B - B_0)^{-1}$ in its vicinity. In the 2D context a Fano–Feschbach resonance has been used[26] to tune the coupling strength $\tilde{g}$ of a cesium gas between 0.05 and 0.26.

1.2.4. *Direct implementation of the XY model*

Most of this chapter is devoted to the description and the analysis of experiments performed with continuous 2D atomic gases. Here we briefly describe another cold-atom setup[31] that can be viewed as an atomic realisation of a 2D array of Josephson junctions, and thus constitutes a direct implementation of the XY model. The experiment starts with a regular hexagonal array of parallel tubes created in a 2D optical lattice. Each tube can be labelled by its coordinates i, j in the plane perpendicular to the tube axis. It contains a large number of atoms forming a condensate, which can be described by a classical complex field ψ_{ij}. In this limit the amplitude $|\psi_{ij}|$ can be considered as constant and the only relevant dynamical variable is the phase of the field θ_{ij}. The tunnelling between adjacent tubes, described by the matrix element J, is equivalent to the coupling across a Josephson junction. The phase pattern θ_{ij} is probed by turning off the lattice, which allows neighbouring condensates to merge and interfere. In particular vortices in the initial phase distribution of the tubes are converted into density holes of the recombined condensate. The measurements of the surface density of these vortices reveal that it is a function of the ratio J/T only, and this function is in good agreement with the BKT prediction.

1.3. Theoretical understanding of interacting atomic gases

We present in this section the main features of an atomic 2D Bose gas, restricting ourselves to the regime where interactions can be described by the dimensionless, energy-independent parameter $\tilde{g}$ given in Eq. (1.3). We first discuss the equation of state of a uniform gas and we comment on its various regimes. We then turn to the case of a harmonically trapped gas and show how this situation can be addressed using local density approximation. Finally we contrast the prediction of a superfluid BKT transition in the central region of the trap with that of a standard Bose–Einstein condensation, as expected for an ideal gas.

1.3.1. *The equation of state of a homogeneous 2D Bose gas*

The equation of state of a fluid consists in the expression of relevant state variables, such as the phase space density, in terms of other variables such as the chemical potential μ and the temperature T. Taking the ideal Bose gas as an example,[13] we can write its phase space density $\mathcal{D}$ as

$$\mathcal{D} \equiv n\lambda^2 = -\ln\left[1 - e^{-\mu/k_{\mathrm{B}}T}\right], \tag{1.5}$$

where $\lambda = (2\pi\hbar^2/mk_{\mathrm{B}}T)^{1/2}$ is the thermal wavelength.

The approximation that consists in describing the interactions in terms of the dimensionless parameter $\tilde{g}$ entails that the equation of state of the 2D gas $\mathcal{D}(\mu, T, \tilde{g})$ must present a scale invariance[32] : since $\mathcal{D}$ is dimensionless, it cannot be an arbitrary function of the two variables μ and $k_{\mathrm{B}}T$ and it can depend only on the ratio of

these two quantities. This (approximate) scale invariance occurs for all interaction strengths $\tilde{g} \ll 1$ and is specific to the two-dimensional case.

The determination of the function $\mathcal{D}(\mu/k_{\rm B}T, \tilde{g})$ for arbitrary values of $\mu/k_{\rm B}T$ requires a numerical calculation. Prokof'ev and Svistunov[32] computed it for $\tilde{g} \ll 1$ using a classical field Monte Carlo method. Two limiting cases can be recovered analytically. In the regime $\mathcal{D} \lesssim 1$, one can use the Hartree–Fock approximation[33]: interactions are treated at the mean-field level and each particle acquires the energy $2gn$ from its interaction with the neighbouring atoms. The factor 2 here is due to the exchange term in the Hartree–Fock approach[a]; it reflects the fact that in the non-degenerate limit, bosons are bunched and $\langle n^2 \rangle = 2n^2$. We then replace μ by $\mu + 2gn$ in the ideal gas result (1.5) and obtain:

$$\mathcal{D} \lesssim 1 : \quad \mathcal{D} \approx -\ln\left[1 - e^{-\mu/k_{\rm B}T} e^{-\tilde{g}\mathcal{D}/\pi}\right]. \tag{1.6}$$

In practice this approximate form of the equation of state is used to determine the value of T and μ of the trapped gas, exploiting, via the local density approximation, the spatial variation of the atomic distribution at the edges of the cloud.

The opposite regime of a strongly degenerate gas can also be handled analytically. This is the so-called *Thomas–Fermi regime*, in which density fluctuations are suppressed ($\langle n^2 \rangle = n^2$) and kinetic energy is negligible. The only relevant energy is due to interactions, so that $\mu = gn$ or equivalently

$$\mathcal{D} \gg 1 : \quad \mathcal{D} = \frac{2\pi}{\tilde{g}} \frac{\mu}{k_{\rm B}T}. \tag{1.7}$$

1.3.2. *The superfluid transition*

Vortex pairing. For a large enough phase space density, the interacting Bose gas is expected to become superfluid with a transition that is of the BKT type. We briefly summarise the physical mechanism[6,7] at the heart of the transition, *i.e.* vortex pairing. Let us first assume that density fluctuations are essentially frozen in the gas, so that the dynamics is dominated by thermal phase fluctuations. We shall return to this assumption later in this section. Among possible sources for phase fluctuations, vortices play an essential role. For simplicity we consider only vortices with unit topological charge, for which the local phase of the fluid has a winding of $\pm 2\pi$ around the vortex core. For a temperature below the transition point, the free energy of an isolated vortex is positive and infinite in the thermodynamic limit. In this regime vortices can only exist in the form of bound pairs, containing two vortices of opposite circulation (figure 1.1). The one-body correlation function $g_1(r)$ decays algebraically at long distance, $g_1(r) \propto r^{-\alpha}$, and a non-zero superfluid density $n_{\rm s}$ can appear in the fluid. The superfluid density can be related to the exponent characterizing the decay of g_1: $\alpha = 1/\mathcal{D}_{\rm s}$, where $\mathcal{D}_{\rm s} = n_{\rm s}\lambda^2$. For a given total density n, the average distance between the two members of a pair is an increasing

[a]The same factor of 2 occurs in the description of the Hanbury-Brown and Twiss effect.

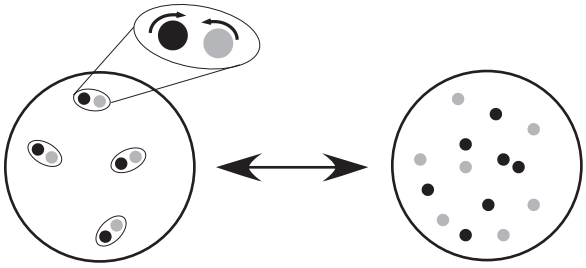

Fig. 1.1. Vortices exist in a two-dimensional Bose gas as possible thermal excitations. Left: in the thermodynamic limit and for a temperature below the critical point, vortices can only exist in the form of bound pairs with a total zero circulation. The gas has a non-zero superfluid component. Right: for a temperature larger than the critical point, the proliferation of free vortices brings the superfluid fraction to zero.

function of temperature. There exists a critical temperature at which this distance diverges, signalling a proliferation of free vortices. This plasma of free vortices, with positive and negative circulations, destroys superfluidity so that $n_{\rm s}$ is zero above the critical point.

The critical point for the superfluid transition. One can show that the superfluid phase space density $\mathcal{D}_{\rm s} = n_{\rm s}\lambda^2$ undergoes a universal jump at the transition point[34]

$$\mathcal{D}_{\rm s} = 4 \longrightarrow \mathcal{D}_{\rm s} = 0 \; . \tag{1.8}$$

This remarkable result is independent of the strength of interactions $\tilde{g}$. Note that this is an implicit result that does not allow one to determine unambiguously the position of the critical point. Indeed the total phase space density $\mathcal{D}$ and the temperature T in (1.8) are at this point still unknown, and the only information is the obvious inequality $\mathcal{D} > 4$.

Numerical calculations[32] indicate that the *total* phase space density $\mathcal{D}$ is a smooth function of $\mu/k_{\rm B}T$ around the critical point. It shows no direct signature of the BKT phase transition, which is in line with the fact that this transition is of infinite order. Using a calculation of the superfluid density via a classical Monte Carlo simulation, Prokofev *et al.*[35] have determined the position of this critical point for $\tilde{g} \ll 1$

$$\mathcal{D}^{\rm crit.} \approx \ln(380/\tilde{g}), \qquad \frac{\mu^{\rm crit.}}{k_{\rm B}T} \approx \frac{\tilde{g}}{\pi}\ln(13.2/\tilde{g}). \tag{1.9}$$

This result complements analytical predictions[36] obtained earlier for asymptotically low values of $\tilde{g}$. In the vicinity of the critical point, the behavior of the system is universal[32] in the sense that $\mathcal{D} - \mathcal{D}^{\rm crit.}$ is a function of the single parameter $(\mu - \mu^{\rm crit.})/(\tilde{g}\, k_{\rm B}T)$.

Density fluctuations. An important ingredient for the BKT mechanism to operate in an atomic gas is the reduction of density fluctuations for phase space densities $\mathcal{D}$ around $\mathcal{D}^{\rm crit.}$. For $\mathcal{D} < \mathcal{D}^{\rm crit.}$, the gas with reduced density fluctuations constitutes a presuperfluid medium, in which the dynamics is essentially governed by the phase fluctuations dynamics. We quote again the results of the classical field Monte Carlo calculation:[35]

$$\frac{n_{\rm qc}}{n} = \frac{7.16}{\ln(380/\tilde{g})} \tag{1.10}$$

at the critical point. Here the "quasi-condensate" density $n_{\rm qc}$, defined by $n_{\rm qc}^2 = 2n^2 - \langle n^2 \rangle$, captures the reduction of density fluctuations: (i) $n_{\rm qc}$ vanishes in the ideal gas limit where atom bunching leads to $\langle n^2 \rangle = 2n^2$. (ii) $n_{\rm qc} = n$ when density fluctuations are negligible ($\langle n^2 \rangle = n^2$). The result (1.10) shows that for practical values of $\tilde{g}$ in atomic physics (say larger than 0.01), the quasi-condensate density is close to the total density. One therefore expects that density fluctuations are strongly suppressed in the vicinity of the transition point. Note that with this definition, the notion of a quasi-condensate makes no direct reference to the coherence properties of the gas.

1.3.3. *The case of trapped gases*

The local density approximation. Experiments with atomic gases are mostly performed in the presence of a harmonic confinement $V(\boldsymbol{r})$ in the xy plane. The local density approximation (LDA) amounts to assuming that the thermodynamic variables of the gas at any point $\boldsymbol{r}$ in the trap, such as the phase space density $\mathcal{D}(\boldsymbol{r})$, take the same value as in a homogenous system with the same temperature T and a chemical potential $\mu - V(\boldsymbol{r})$. Therefore, instead of being a nuisance, the non-homogeneity of the trapping potential is often an asset; it provides in a single-shot measurement the equation of state of the fluid for chemical potentials ranging from $-\infty$ (at the edges of the cloud) to μ (in the centre).

The LDA is valid if the various thermodynamic quantities do not change significantly over the length scales set by the healing length ξ, the thermal wavelength λ and the characteristic size of the ground state of the single particle motion in the xy plane $a_{xy} = [\hbar/(m\omega_{xy})]^{1/2}$. It can be tested experimentally by measuring at given T the radial density distributions of the gas for several values of the particle number, hence several values of the chemical potential (μ_j) , and by checking that all distributions get superimposed when plotted as function of $\mu_j - V(r)$. LDA was also validated using Quantum Monte Carlo simulations.[37] These simulations were performed for a number of bosons and a trap geometry comparable to the experimental parameters, taking into account in particular the residual excitation of the z degree of freedom. The superfluid fraction was obtained from the value of the non-classical moment of inertia. The results were in good agreement with the predictions[32] for a homogenous system combined with LDA, and the small residual deviations have been analysed by various authors.[38–41]

The competition between BKT physics and Bose–Einstein condensation. The simple fact of placing the atomic gas in a trap immediately raises the question of possible finite-size effects. This question also emerges for 3D trapped gases, but it is even more relevant in 2D since it is well known that approaching the thermodynamic limit is an extremely difficult task in this case. In the context of 2D magnetism, Bramwell and Holdsworth[42] wrote the famous statement: "With a magnetization at the BKT critical point smaller than 0.01 as a reasonable estimate for the thermodynamic limit, the sample would need to be bigger than the state of Texas for the Mermin–Wagner theorem to be relevant!" Needless to say, cold atomic gases are very far from this limit. The ratio between the characteristic size of the gas and the microscopic lengths ξ and λ does not exceed a few hundreds, and finite size effects cannot be ignored.

The situation is made even more intricate by the presence of the harmonic confinement $V(r) = m\omega^2 r^2/2$ in the xy plane (in this section we set $\omega \equiv \omega_{xy}$ for simplicity). In the ideal gas case where no BKT transition is expected, an assembly of bosons can undergo a standard Bose–Einstein condensation (BEC) in the thermodynamic limit,[43] where $N \to \infty$, $\omega \to 0$, with $N\omega^2$ kept constant. The BEC transition takes place when the temperature is below the critical value

$$k_{\rm B} T_{\rm ideal}^{\rm crit.} = (\sqrt{6}/\pi)\, \hbar\omega\, N^{1/2}, \tag{1.11}$$

or equivalently when N exceeds the critical atom number

$$N_{\rm ideal}^{\rm crit.} = (\pi^2/6)(k_{\rm B} T/\hbar\omega)^2 \tag{1.12}$$

for a gas maintained at fixed temperature T. This result can be inferred from (1.5) by (i) replacing μ by the local chemical potential $\mu - V(r)$ in the expression for the density:

$$n(r)\lambda^2 = -\ln\left[1 - e^{-[\mu - V(r)]/k_{\rm B}T}\right], \tag{1.13}$$

(ii) requiring that the chemical potential is equal to $V(0) = 0$ at the condensation point, and (iii) calculating $N = \int n\, d^2 r$.

We now switch to the case of an interacting Bose gas in a harmonic potential, and meet the natural question: when increasing the atom number in a gas at fixed temperature, what is (are) the phase transition(s) that one may encounter: a Bose–Einstein transition, with a possible shift of the critical atom number with respect to (1.12), or (and) a BKT-driven transition? To address this question, we first recall the simpler 3D case. In a uniform ideal gas, BEC occurs at the density $n_{3,\,\rm ideal}^{\rm crit} = 2.612\, \lambda^{-3}$. In a harmonically confined ideal gas, BEC occurs when the density at the center reaches the same threshold, which requires the presence of $N_{3,\,\rm ideal}^{\rm crit.} = 1.202\, (k_{\rm B} T/\hbar\omega)^3$ atoms in the trap. In the presence of weak repulsive interactions, BEC occurs for (approximately) the same central density[1] $n_{3,\,\rm ideal}^{\rm crit}$. Achieving this density requires to put more atoms in the trap than in the ideal case since repulsion between atoms tends to broaden the spatial distribution. Therefore

in the 3D case, the main effect of interactions is[1] an upwards shift of the critical atom number with respect to $N_{\rm ideal}^{\rm crit.}$ at fixed T, or equivalently a downwards shift of the critical temperature with respect to $T_{\rm ideal}^{\rm crit.}$ at fixed N.

In the 2D case, the ideal gas BEC in a harmonic trap is a marginal and fragile effect, in the sense that it is associated with an infinite spatial density n (hence an infinite phase space density $\mathcal{D}$) in the center. This result is a direct consequence of Eq. (1.13) when one lets $\mu \to 0$. Now in the presence of repulsive interactions between atoms, the divergence of the spatial density in the center cannot occur anymore, and one cannot hope to recover a situation similar to the ideal case by simply increasing the atom number. Therefore our first conclusion is that for a 2D trapped gas, the standard BEC does not survive in the presence of interactions, at least when the discrete nature of the single-particle eigenstates can be omitted (i.e. when $k_{\rm B}T \gg \hbar\omega$).

On the other hand the BKT superfluid transition requires a non-infinite phase space density to occur, and we thus expect that it can still take place in a trapped Bose gas with repulsive interactions. To determine in which conditions this transition is observable, we can rely on LDA. We use Eq. (1.9) to provide the density threshold $n^{\rm crit} = \ln(380/\tilde{g})\,\lambda^{-2}$ at which the gas in the center of the trap becomes superfluid. Using the Hartree–Fock result (1.6), this criterion can be transposed[44] into the critical atom number[b]

$$N_{\rm BKT}^{\rm crit.} = N_{\rm ideal}^{\rm crit.}\left[1 + \frac{3\tilde{g}}{\pi^3}\left(\mathcal{D}^{\rm crit.}\right)^2\right]. \tag{1.14}$$

It is noteworthy that the critical atom number for observing a BKT transition in a harmonic trap has the same scaling with respect to T and ω as the critical number for BEC of an ideal gas. In addition Eq. (1.14) implies that the BKT threshold for an interacting gas requires more particles than the BEC threshold for an ideal gas at the same temperature.

To summarise we expect that a single, BKT-driven, phase transition takes place in a trapped interacting 2D gas.[13] When taking the limit $\tilde{g} \to 0$, the critical phase space density $\mathcal{D}^{\rm crit.}$ given in Eq. (1.9) for a uniform system tends to infinity, and the critical atom number $N_{\rm BKT}^{\rm crit.}$ for a trapped gas tends to the ideal gas threshold (1.12) for BEC. The ideal gas BEC in a 2D harmonic potential can thus be viewed as a special, non-interacting limit of the BKT transition. We also note that in the presence of interactions, there exists in addition to the BKT transition a cross-over in which the density fluctuations gradually decrease. As for the homogeneous case this cross-over mostly takes place for phase space densities lower than $\mathcal{D}^{\rm crit.}$, and it produces a presuperfluid medium in which the BKT mechanism can operate.

The condensed fraction. Because of finite-size effects, the conclusion that we just reached concerning the non-existence of a standard BEC transition is still

[b]Note that Eq. (1.14) is an upper bound on $N_{\rm BKT}^{\rm crit.}$ because it assumes that the interaction energy per particle is $2gn$. It is in reality smaller due to the reduction of density fluctuations.

compatible with a significant condensed fraction in the trapped gas. The condensed fraction Π_0 is defined as the largest eigenvalue of the one-body density matrix $\hat{\rho}$, with $\langle \boldsymbol{r}|\hat{\rho}|\boldsymbol{r}'\rangle = g_1(|\boldsymbol{r}-\boldsymbol{r}'|)$ in a uniform system. When $g_1(r)$ is significantly different from zero for values of r comparable to the characteristic radius of the trapped gas R, then we expect that this gas exhibits a detectable macroscopic quantum coherence.

Let us first address the case where the superfluid threshold (1.14) has been reached and suppose that R stands for the radius of the disk where the superfluid fraction is non-zero. Since g_1 decays algebraically in the superfluid region with an exponent that is smaller than $1/4$, we have $\Pi_0 \approx g_1(R) \gtrsim (\xi/R)^{1/4}$. The radius R can be estimated using the Thomas–Fermi approximation[1]: in the limit where the kinetic energy is negligible, the spatial density $n(r)$ in the superfluid disk is obtained from the simple relation $gn(r) + V(r) = \mu$, hence $R = a_{xy}(4\tilde{g}N/\pi)^{1/4}$, where N is the number of atoms in the disk. Taking as typical values $a_{xy} = 3\,\mu$m, $\tilde{g} = 0.1$, $N = 2\,10^4$, we find $R \approx 20\,\mu$m. The healing length in the center of the trap ξ is $\approx 0.6\,\mu$m, so that $\Pi_0 \gtrsim 0.4$.

The emergence of a detectable condensed fraction can significantly precede the point where the critical density (1.9) is reached in the center of the trap. This is due to the particular behaviour of the correlation length ℓ characterising the exponential decay of g_1 in the normal (non-superfluid) region. In a uniform 2D fluid, the length ℓ is predicted to diverge exponentially at the critical point ($\ell \sim \exp[b/(T - T_c)^{1/2}]$, where b is a constant), hence ℓ may take a value comparable to the size R of the trapped cloud notably before the threshold (1.14) is reached. One can thus predict that the transition from a fully thermal to a significantly coherent gas is actually a crossover, whose relative width $\Delta T/T_c$ ranges from 5% to 20% for realistic trap parameters.[13] An evidence for this crossover is provided by classical field Monte Carlo calculations for a trapped gas.[45,46]

1.4. Experimental investigation of 2D physics in atomic gases

In ultracold atom research essentially all raw data take the form of images of atomic clouds. The most commonly used technique is absorption imaging, whereby a laser beam tuned close to resonance with an atomic transition is passed through the cloud, and the "shadow" of the cloud is imaged on a camera. From the fractional attenuation of the laser beam at any point in the image plane, one infers the column atomic density along the "line of sight" of the laser. While this probe always couples to the atomic density, what the observed density distribution actually represents depends on what one does with the atomic cloud just before imaging it. We can distinguish three typical scenarios which are relevant for our discussion here:

(1) If one takes an image of a trapped atomic cloud then one indeed simply obtains the (column) density distribution.

(2) In the "time of flight" (TOF) technique, the cloud is released from the trap some time before the image is taken, and the atoms are allowed to freely expand. For

sufficiently long expansion times (typically tens of milliseconds), the cloud becomes significantly larger than its initial in-trap size. In this limit the observed density distribution reflects the *momentum* distribution of the atoms.

(3) Finally, in matter-wave interference experiments, two initially separate clouds, or two parts of the same cloud, are made to overlap during the expansion. In this way the phase properties of the wave function(s) describing the cloud(s) are converted into density information which can be extracted by imaging. This option is particularly appealing for studies of 2D physics since it allows direct visualisation of both phonons and vortices, as well as quantitative measurements of correlation functions.

1.4.1. *Measurements of density and momentum distributions*

An obvious way to experimentally obtain the equilibrium density distribution of a trapped 2D gas is to take an absorption image along the direction (z) perpendicular to the planar gas. In contrast to the case of a 3D gas, in the 2D case the line-of-sight integration by the imaging beam does not result in any loss of information, since along z the gas is simply in the ground-state of the trapping potential $U(z)$.

Besides the average density distribution, one can in principle in this way also study the density fluctuations which are suppressed in the degenerate regime. Moreover, taking advantage of the non-uniform density profile in a harmonic trap, from the spatial variation of the (average) density one can deduce the compressibility of the gas, and hence quantify the level of density fluctuations in that way. Qualitatively, the compressibility of the gas is directly related to the interaction energy density, and hence reveals whether $\langle n^2 \rangle$ is closer to $2\langle n \rangle^2$ (corresponding to a fully fluctuating gas) or to $\langle n \rangle^2$ (corresponding to suppressed density fluctuations).

The in-trap density measurements however do not provide information on the phase fluctuations, neither phonons nor vortices. Vortices in principle do have a signature in the density distribution, but in practice the size ξ of a vortex core is smaller than a micrometer, which is usually too small compared to the imaging resolution to be directly observed.

To measure the momentum distribution one can use the time-of-flight (TOF) technique. In it simplest version a TOF measurement entails a sudden switch-off of all confining potentials, and a subsequent expansion of the gas along all three spatial dimensions ("3D TOF"). For studies of 2D gases this technique has two qualitatively different variants:

- One can choose to turn off only the confining potential $V(r)$ in the xy plane, while leaving the tight confinement $U(z)$ on during the expansion. In this "2D TOF" approach the gas lives in two dimensions at all times.
- One can switch off the confinement $U(z)$ along the initially strongly confined direction z, while keeping the potential $V(r)$ in the xy plane ("1D TOF").

After long TOF, the observed density distribution reflects the momentum dis-

tribution in the cloud. However, this momentum distribution is in general not the same as the original momentum distribution in a trapped gas. The reason for this is that the interaction energy of a trapped gas is converted into (additional) kinetic energy during the early stages of the expansion. We can now already anticipate that this conversion of interaction into kinetic energy is different if the gas expands along one, two or three directions.

***In situ* images.** A series of experiments have investigated the equilibrium state of an atomic 2D Bose gas using in-trap images.[25,26,47] The measured density profiles are in good agreement with the prediction of classical field Monte Carlo calculations, associated with LDA. The scale invariance of the equations of state for the phase space density[26]and the pressure[47] of the gas have been confirmed, which also allows one to deduce the equation of state for the entropy of the gas.[47] In addition one can extract from these measurements the compressibility of the gas[25,26] and thus directly confirm the suppression of the density fluctuations.

It is important to stress that in these *in situ* measurements, nothing remarkable happens at the BKT transition point when the atom number reaches $N_{\rm BKT}^{\rm crit.}$. Also for an atom number well above this critical value, the average density distribution varies smoothly in space, including around the radius r where the phase space density equals the critical value (1.9). As already mentioned this absence of singularity is a consequence of the fact that the BKT transition is of infinite order.

2D TOF. In 2D TOF something remarkably simple happens - the density distribution evolves in a self-similar way[48] and the picture of the cloud simply gets rescaled. Explicitly, if the equilibrium in-trap density profile is $n_{\rm eq}(\boldsymbol{r})$, then in 2D TOF we get:

$$n(\boldsymbol{r},t) = \eta_t^2\, n_{\rm eq}(\eta_t \boldsymbol{r}) \ \text{, where } \ \eta_t = (1+\omega^2 t^2)^{-1/2} \ , \tag{1.15}$$

where t is the expansion time. Such perfect scaling is a direct consequence of the fact that the coupling strength $\tilde{g}$ is a dimensionless constant, and it entails that purely 2D measurements in principle provide identical information, whether they are performed in-trap or in 2D TOF.

An evidence for this scaling has been obtained experimentally.[17] Small deviations (not yet observed) are expected[49,50] because of the logarithmic dependence of the coupling strength with respect to the energy of the particles (Eq. (1.4)), which itself results from the needed regularisation of the contact interaction potential in 2D.

1D and 3D TOFs. 1D and 3D TOFs provide a way to observe directly the occurrence of the BKT transition in a trapped gas. Indeed in this case the high trap anisotropy results in an expansion of the cloud along z in a time $\sim \omega_z^{-1}$ that is short compared to any time constant associated with the motion in the xy plane.

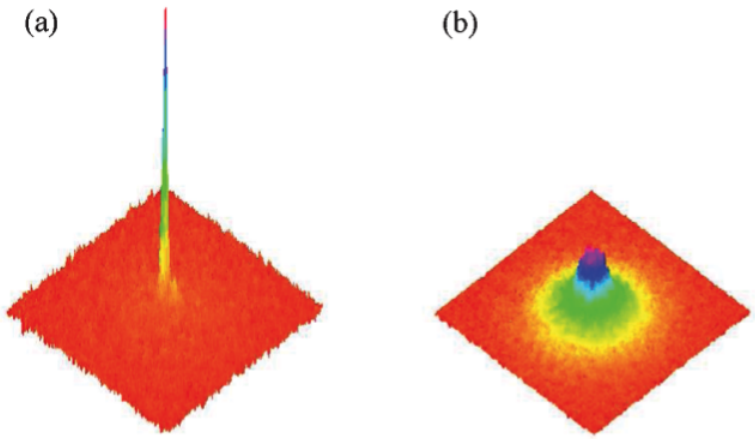

Fig. 1.2. (a) Momentum distribution of a 2D Bose gas, for an atom number above the critical value. (b) *In situ* density distribution for near-identical conditions (image from reference[25] courtesy of Eric Cornell).

We can then conceptually divide the expansion into two stages: in the initial stage all the interaction energy is taken out of the system by the fast expansion along z, before almost any motion of the atoms in the xy plane occurs, and without affecting the in-plane momentum distribution. The subsequent slower in-plane evolution of the density distribution thus corresponds either to the evolution in the potential $V(r)$ (1D TOF) or to the free expansion of an ideal gas (3D TOF). In both cases, the initial momentum distribution is the same as the trapped gas.

With both methods one observes that the momentum distribution becomes sharply peaked for atom numbers above a critical value which is in good agreement with the BKT prediction[15,25,51] (see *e.g.* fig. 1.2 (a)). Since the momentum distribution is the Fourier transform of g_1, this sharp peak signals the appearance of a significant condensed fraction, with a phase ordering that extends over a large fraction of the trapped cloud. The signalling of the BKT transition via the appearance of this sharp peak in momentum space is very reminiscent of the emergence of a non-zero magnetisation at the BKT critical point for a finite size XY system.[42]

In the context of cold atomic gases, it is particularly interesting to perform both in-trap and 1D/3D TOF density/momentum measurements on identically prepared samples.[25] In this case the 1D/3D measurements provide the striking qualitative signature of the phase transition (fig. 1.2 (a)), while the in-trap measurements (fig. 1.2 (b)) allow quantitative confirmation that the condensate momentum peak emerges at the critical phase space density predicted by the BKT theory.

1.4.2. *Visualising phase fluctuations*

To directly visualise the phase fluctuations in a 2D Bose gas, both the phonons which (in the thermodynamic limit) destroy the LRO even at very low T, and the vortices which drive the BKT transition, in atomic physics one can employ matter-wave interference experiments. It is in principle possible to interfere two different parts of the same 2D sample,[15] but here we will illustrate the key ideas by considering the more intuitive case of interference between two parallel, independent 2D clouds.[24] This scenario is illustrated in figure 1.3.

We consider two planes of atoms which are separated by a distance d_z along z. The potential barrier between the planes is sufficiently large so that there is no quantum tunnelling between the two planes and the phase fluctuations in them are independent. At the same time the planes can be considered to be statistically identical, i.e. they have very similar temperature and atomic density. Such a configuration can readily be realised in a one-dimensional optical lattice, as explained in section 1.2.1. Each plane (a, b) is thus described by the wave function $\psi_{a/b}(x, y) = |\psi_{a/b}|e^{i\theta_{a/b}(x,y)}$, where $|\psi_a| \approx |\psi_b|$, while $\theta_a(x, y)$ and $\theta_b(x, y)$ are independently fluctuating.

If we perform a 3D TOF of sufficiently long duration t, the two clouds expand into each other and interfere. Moreover, there exists an intermediate range of times t for which we can still assume that no expansion in the xy plane has taken place. In this way we obtain an interference pattern in which the local interference phase depends on the local difference $\theta_a(x, y) - \theta_b(x, y)$. More explicitly, neglecting the trivial global envelope function (which describes the expansion along z of each cloud) the total density distribution after TOF is:

$$n \propto |\psi_a|^2 + |\psi_b|^2 + \left(\psi_a \psi_b^* \, e^{i2\pi z/D_z} \; + \; \text{c.c.}\right) \, , \tag{1.16}$$

where $D_z = ht/md_z$ is the constant period of the interference fringes. In practice this density distribution is then projected onto the xz plane by absorption imaging along the y direction.

Phonons. At very low T the functions θ_a and θ_b are almost constant, and hence so is their difference. Although this difference is not known, or even defined, prior to the actual measurement, the interference of two such planes with quasi-constant phases inevitably leads to straight interference fringes, as shown in figure 1.3 (b). The absolute difference between θ_a and θ_b simply corresponds to the absolute position (along z) of the fringes on the camera, and varies randomly between different experimental realisations.

On the other hand if the phase describing each plane slowly varies in space, this results in the meandering interference pattern, such as shown in figure 1.3 (c). Experimentally it is observed that the fringes indeed gradually become more wavy as the temperature is increased.

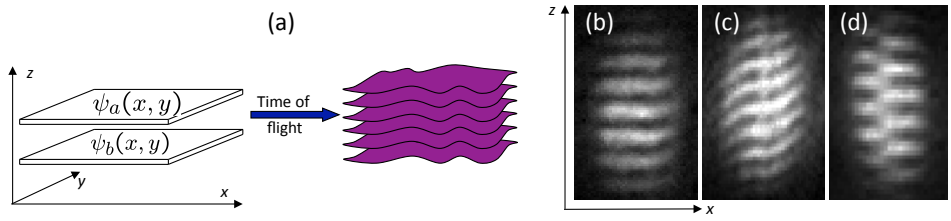

Fig. 1.3. (a) Principle of an experiment in which two independent 2D Bose gases, described by fluctuating macroscopic wave functions ψ_a and ψ_b, are released from the potential that was initially confining them along the z direction. The overlap of the expanding matter waves leads to interference patterns that are observed by looking at the absorption of a probe laser beam. (b-d) Examples of observed interference patterns.[24] The contrast and the waviness of the patterns provide information on the phase distributions of the initial states $\psi_{a,b}$.

Vortices. An important outcome of the experiments[24] depicted in figure 1.3 is the direct visual evidence for the proliferation of free vortices near the BKT transition. If a free vortex is present in one of the two interfering clouds, while the phase of the other cloud varies smoothly across the same region in the xy plane, the vortex appears as a sharp dislocation in the interference pattern. An example of such a dislocation is shown in figure 1.3 (d). The reason for the dislocation is that as one moves along x, the relative phase $\theta_a - \theta_b$ suddenly jumps by π at the position of the vortex.

These π-dislocations are absent at low temperature and the probability of their occurrence rapidly rises as one approaches the BKT critical temperature from below. Once the critical temperature is crossed and the gas becomes strongly (phase-) fluctuating, the interference pattern is no longer observable.

1.4.3. *Correlation functions*

From two-plane interference experiments one can also extract off-diagonal correlation functions, by studying the spatial variation of the phase of the complex interference contrast in eq. (1.16).

A particularly elegant method for quantitative analysis of correlation functions was proposed by Polkovnikov *et al.*,[52] and we outline it here. As we mentioned above, the interference pattern can never be measured at a single point in the xy plane, but is always integrated by imaging along y. Additionally one can choose to integrate it over an arbitrary distance along x. Qualitatively, we can see that the contrast of the resulting integrated image will decay with the integration area whenever the fringes show some phase fluctuations. The more fluctuating the gases are, the more rapid will the decay of the contrast be. More quantitatively, we can define an average integrated contrast, obtained by averaging over many experimental

realisations:

$$\mathcal{C}^2(A) = \frac{1}{A^2}\left\langle \left| \int_A \psi_a(\boldsymbol{r})\psi_b^*(\boldsymbol{r})\, d^2r \right|^2 \right\rangle \quad , \tag{1.17}$$

where A is the integration area, which here we assume to be square. Since ψ_a and ψ_b are uncorrelated and have statistically identical fluctuations, for a uniform system this factors out to yield:

$$\mathcal{C}^2(A) = \frac{1}{A}\int_A |g_1(\boldsymbol{r})|^2\, d^2r \ , \tag{1.18}$$

where $g_1(\boldsymbol{r})$ is the first order correlation function describing either of the two planes. Similarly, from higher moments of the distribution of $\mathcal{C}^2(A)$ one can extract higher order correlation functions.

Focusing on the first order correlation function, we can distinguish two qualitatively different cases. In the normal state g_1 is rapidly (exponentially) decaying, so for sufficiently large A we get $\mathcal{C}^2(A) \propto A^{-1}$. On the other hand, in the superfluid state g_1 decays only slowly (algebraically), $g_1 \propto r^{-\alpha}$, with $\alpha = 1/(n_s\lambda^2)$. We thus get $\mathcal{C}^2(A) \propto A^{-2\alpha}$. Since $\alpha \leq 1/4$, at the BKT transition the exponent characterising the decay of $\mathcal{C}^2(A)$ jumps between 1 and 1/2. This jump corresponds to the universal jump in the superfluid density,[52] and is a direct coherence analogue of the jump observed in the transport experiments with liquid helium films.[8]

Although adapting these calculations to a harmonically trapped gas is a difficult task,[53] one can use eq. (1.18) as a qualitative guide. Experimental measurements of $\mathcal{C}^2(A)$ indeed qualitatively agree with the expected change from exponential to algebraic decay of g_1 in the vicinity of the BKT transition temperature.[24] Specifically, within experimental precision, this change coincides with the proliferation of interference defects signalling the presence of free vortices in 2D clouds.

1.5. Outlook

So far we have advertised the measurements performed with 2D atomic gases as complementary to those performed on other physical systems displaying BKT physics. In particular, at the level of theory, coherence measurements on atomic systems are a direct analogue of the transport measurements on liquid helium films. It is however important to also stress that superfluidity in the traditionally defined transport sense has not yet been observed in these systems. In fact, a quantitative measurement of the superfluid density is more generally an open question in the field of ultracold atomic gases. This is an active area of current research,[54,55] and one big hope is that in the near feature it will be possible to perform both types of measurements on identically prepared atomic samples, thus providing a direct experimental comparison of different theoretical definitions of superfluidity.

To conclude, we briefly mention two further experimental possibilities that have recently emerged in the field of ultracold atomic gases, and could in the future be

applied to 2D systems:

First, atomic gases are naturally very "clean", but it is possible to controllably introduce various degrees of disorder into these systems.[56] A particularly flexible approach is to use either quasi-periodic or truly random optical potentials, so that the strength of the disordered potential is simply proportional to the laser intensity. In the case of random, laser speckle potentials, the disorder can be truly microscopic in the sense that the correlation length of the random potential can be comparable to the healing length ξ. Recently, application of optically induced disorder allowed studies of Anderson localisation[57,58] in clouds close to zero temperature. In the future it should be equally possible to apply similar techniques to 2D gases at non-zero temperature in order the study the effects of disorder on the BKT transition.

Second, atomic gases exhibit comparatively slow dynamics, with characteristic timescales ranging from milliseconds to seconds; this allows real-time studies of dynamical effects, such as transient regimes following a quench of some Hamiltonian parameter. In the context of BKT physics, one could for example study the emergence of superfluidity after suddenly crossing the critical point by changing the strength of interactions in the gas. Moreover, theoretical analogies between the evolution (decay) of coherence in real space and in time have been proposed.[59] In a bi-layer system such as that introduced in section 1.4.2, one can dynamically control the strength of tunnel-coupling between the two planes, so that the phases of their wave functions are initially locked together and then suddenly decoupled. By studying the interference of the two planes at various times after the quench one could then study the evolution of their relative phases under the influence of thermal fluctuations. In the superfluid regime, the integrated interference contrast is expected to decay algebraically at long times, as $t^{-\zeta}$ with $\zeta \propto T$, in analogy with the spatial decay of the first order correlation function g_1 in an equilibrium 2D gas.

References

1. F. S. Dalfovo, L. P. Pitaevkii, S. Stringari, and S. Giorgini, Theory of Bose–Einstein condensation in trapped gases, *Rev. Mod. Phys.* **71**, 463 (1999).
2. M. Lewenstein, A. Sanpera, V. Ahufinger, B. Damski, A. S. De, and U. Sen, Ultracold atomic gases in optical lattices: mimicking condensed matter physics and beyond, *Adv. Phys.* **56**, 243 (2007).
3. I. Bloch, J. Dalibard, and W. Zwerger, Many-body physics with ultracold gases, *Rev. Mod. Phys.* **80**, 885 (2008).
4. S. Giorgini, L. P. Pitaevskii, and S. Stringari, Theory of ultracold atomic Fermi gases, *Rev. Mod. Phys.* **80**, 1215 (2008).
5. N. R. Cooper, Rapidly rotating atomic gases, *Advances in Physics.* **57**, 539 (2008).
6. V. L. Berezinskii, Destruction of long-range order in one-dimensional and two-dimensional system possessing a continous symmetry group - ii. quantum systems, *Soviet Physics JETP.* **34**, 610 (1971).
7. J. M. Kosterlitz and D. J. Thouless, Ordering, metastability and phase transitions in two dimensional systems, *J. Phys. C: Solid State Physics.* **6**, 1181 (1973).

8. D. J. Bishop and J. D. Reppy, Study of the superfluid transition in two-dimensional ^{4}He films, *Phys. Rev. Lett.* **40**, 1727 (1978).
9. C. Chin, R. Grimm, P. Julienne, and E. Tiesinga, Feshbach resonances in ultracold gases, *Rev. Mod. Phys.* **82**, 1225 (2010).
10. N. D. Mermin and H. Wagner, Absence of ferromagnetism or antiferromagnetism in one- or two-dimensional isotropic Heisenberg models, *Phys. Rev. Lett.* **17**, 1133 (1966).
11. P. C. Hohenberg, Existence of long-range order in one and two dimensions, *Phys. Rev.* **158**, 383 (1967).
12. R. Grimm, M. Weidemüller, and Y. B. Ovchinnikov, Optical dipole traps for neutral atoms, *Adv. At. Mol. Opt. Phys.* **42**, 95 (2000).
13. Z. Hadzibabic and J. Dalibard, Two-dimensional Bose fluids: An atomic physics perspective, *Rivista del Nuovo Cimento.* **34**, 389 (2011).
14. A. Görlitz, J. M. Vogels, A. E. Leanhardt, C. Raman, T. L. Gustavson, J. R. Abo-Shaeer, A. P. Chikkatur, S. Gupta, S. Inouye, T. Rosenband, and W. Ketterle, Realization of Bose–Einstein condensates in lower dimensions, *Phys. Rev. Lett.* **87**, 130402 (2001).
15. P. Cladé, C. Ryu, A. Ramanathan, K. Helmerson, and W. D. Phillips, Observation of a 2D Bose gas: From thermal to quasicondensate to superfluid, *Phys. Rev. Lett.* **102**, 170401, (2009).
16. N. L. Smith, W. H. Heathcote, G. Hechenblaikner, E. Nugent, and C. J. Foot, Quasi-2D confinement of a BEC in a combined optical and magnetic potential, *Journal of Physics B.* **38**, 223 (2005).
17. S. P. Rath, T. Yefsah, K. J. Günter, M. Cheneau, R. Desbuquois, M. Holzmann, W. Krauth, and J. Dalibard, Equilibrium state of a trapped two-dimensional Bose gas, *Phys. Rev. A.* **82**, 013609 (2010).
18. C. Orzel, A. K. Tuchmann, K. Fenselau, M. Yasuda, and M. A. Kasevich, Squeezed states in a Bose–Einstein condensate, *Science.* **291**, 2386 (2001).
19. S. Burger, F. S. Cataliotti, C. Fort, P. Maddaloni, F. Minardi, and M. Inguscio, Quasi-2D Bose–Einstein condensation in an optical lattice, *Europhys. Lett.* **57**, 1 (2002).
20. M. Köhl, H. Moritz, T. Stöferle, C. Schori, and T. Esslinger, Superfluid to Mott insulator transition in one, two, and three dimensions, *Journal of Low Temperature Physics.* **138**, 635 (2005).
21. O. Morsch and M. Oberthaler, Dynamics of Bose–Einstein condensates in optical lattices, *Rev. Mod. Phys.* **78**, 179 (2006).
22. I. B. Spielman, W. D. Phillips, and J. V. Porto, The Mott insulator transition in two dimensions, *Phys. Rev. Lett.* **98**, 080404 (2007).
23. Z. Hadzibabic, S. Stock, B. Battelier, V. Bretin, and J. Dalibard, Interference of an array of independent Bose–Einstein condensates, *Phys. Rev. Lett.* **93**, 180403 (2004).
24. Z. Hadzibabic, P. Krüger, M. Cheneau, B. Battelier, and J. Dalibard, Berezinskii–Kosterlitz–Thouless crossover in a trapped atomic gas, *Nature.* **441**, 1118 (2006).
25. S. Tung, G. Lamporesi, D. Lobser, L. Xia, and E. A. Cornell, Observation of the presuperfluid regime in a two-dimensional Bose gas, *Phys. Rev. Lett.* **105**, 230408 (2010).
26. C.-L. Hung, X. Zhang, N. Gemelke, and C. Chin, Observation of scale invariance and universality in two-dimensional Bose gases, *Nature.* **470**, 236 (2011).
27. A. Ramanathan, K. C. Wright, S. R. Muniz, M. Zelan, W. T. Hill, C. J. Lobb, K. Helmerson, W. D. Phillips, and G. K. Campbell, Superflow in a toroidal Bose–Einstein condensate: An atom circuit with a tunable weak link, *Phys. Rev. Lett.* **106**, 130401 (2011).
28. D. S. Petrov, M. Holzmann, and G. V. Shlyapnikov, Bose–Einstein condensation in

quasi-2D trapped gases, *Phys. Rev. Lett.* **84**, 2551 (2000).
29. S. K. Adhikari, Quantum scattering in two dimensions, *American Journal of Physics.* **54**, 362 (1986).
30. D. S. Petrov and G. V. Shlyapnikov, Interatomic collisions in a tightly confined Bose gas, *Phys. Rev. A.* **64**, 012706 (2001).
31. V. Schweikhard, S. Tung, and E. A. Cornell, Vortex proliferation in the Berezinskii–Kosterlitz–Thouless regime on a two-dimensional lattice of Bose–Einstein condensates, *Phys. Rev. Lett.* **99**, 030401 (2007).
32. N. V. Prokof'ev and B. V. Svistunov, Two-dimensional weakly interacting Bose gas in the fluctuation region, *Phys. Rev. A.* **66**, 043608 (2002).
33. L. Kadanoff and G. Baym, *Quantum Statistical Mechanics.* (Benjamin/Cummings Publishing Company, 1963).
34. D. R. Nelson and J. M. Kosterlitz, Universal jump in the superfluid density of two-dimensional superfluids, *Phys. Rev. Lett.* **39**, 1201 (1977).
35. N. V. Prokof'ev, O. Ruebenacker, and B. V. Svistunov, Critical point of a weakly interacting two-dimensional Bose gas, *Phys. Rev. Lett.* **87**, 270402 (2001).
36. D. S. Fisher and P. C. Hohenberg, Dilute Bose gas in two dimensions, *Phys. Rev. B.* **37**, 4936 (1988).
37. M. Holzmann and W. Krauth, Kosterlitz–Thouless transition of the quasi two-dimensional trapped Bose gas, *Phys. Rev. Lett.* **100**, 190402 (2008).
38. M. Holzmann, M. Chevallier, and W. Krauth, Semiclassical theory of the quasi two-dimensional trapped gas, *Europhys. Lett.* **82**, 30001 (2008).
39. M. Holzmann, M. Chevallier, and W. Krauth, Universal correlations and coherence in quasi-two-dimensional trapped Bose gases, *Phys. Rev. A.* **81**, 043622 (2010).
40. Z. Hadzibabic, P. Krüger, M. Cheneau, S. P. Rath, and J. Dalibard, The trapped two-dimensional Bose gas: from Bose–Einstein condensation to Berezinskii–Kosterlitz–Thouless physics, *New Journal of Physics.* **10**, 045006 (2008).
41. R. N. Bisset, D. Baillie, and P. B. Blakie, Analysis of the Holzmann–Chevallier–Krauth theory for the trapped quasi-two-dimensional Bose gas, *Phys. Rev. A.* **79**, 013602 (2009).
42. S. T. Bramwell and P. C. W. Holdsworth, Magnetization: A characteristic of the Kosterlitz–Thouless–Berezinskii transition, *Phys. Rev. B.* **49**, 8811 (1994).
43. V. S. Bagnato and D. Kleppner, Bose–Einstein condensation in low-dimensional traps, *Phys. Rev. A.* **44**, 7439 (1991).
44. M. Holzmann, G. Baym, J. P. Blaizot, and F. Laloë, Superfluid transition of homogeneous and trapped two-dimensional Bose gases, *P.N.A.S.* **104**, 1476 (2007).
45. R. N. Bisset, M. J. Davis, T. P. Simula, and P. B. Blakie, Quasicondensation and coherence in the quasi-two-dimensional trapped Bose gas, *Phys. Rev. A.* **79**, 033626 (2009).
46. R. N. Bisset and P. B. Blakie, Transition region properties of a trapped quasi-two-dimensional degenerate Bose gas, *Phys. Rev. A.* **80**, 035602 (2009).
47. T. Yefsah, R. Desbuquois, L. Chomaz, K. J. Günter, and J. Dalibard, Exploring the thermodynamics of a two-dimensional Bose gas, *ArXiv e-prints: 1106.0188* (2011).
48. L. P. Pitaevskii and A. Rosch, Breathing mode and hidden symmetry of trapped atoms in two dimensions, *Phys. Rev. A.* **55**, R853 (1997).
49. P. O. Fedichev, U. R. Fischer, and A. Recati, Zero-temperature damping of Bose–Einstein condensate oscillations by vortex-antivortex pair creation, *Phys. Rev. A.* **68**, 011602 (2003).
50. M. Olshanii, H. Perrin, and V. Lorent, Example of a quantum anomaly in the physics of ultracold gases, *Phys. Rev. Lett.* **105**, 095302 (2010).

51. P. Krüger, Z. Hadzibabic, and J. Dalibard, Critical point of an interacting two-dimensional atomic Bose gas, *Phys. Rev. Lett.* **99**, 040402 (2007).
52. A. Polkovnikov, E. Altman, and E. Demler, Interference between independent fluctuating condensates, *Proc. Natl. Acad. Sci. USA*. **103**, 6125 (2006).
53. S. P. Rath and W. Zwerger, Full counting statistics of the interference contrast from independent Bose–Einstein condensates, *Phys. Rev. A*. **82**, 053622 (2010).
54. N. R. Cooper and Z. Hadzibabic, Measuring the superfluid fraction of an ultracold atomic gas, *Phys. Rev. Lett.* **104**, 030401 (2010).
55. I. Carusotto and Y. Castin, Non-equilibrium and local detection of the normal fraction of a trapped two-dimensional Bose gas, *ArXiv e-prints: 1103.1818* (2011).
56. L. Sanchez-Palencia and M. Lewenstein, Disordered quantum gases under control, *Nature Physics*. **6**, 87 (2010).
57. G. Roati, C. D'Errico, L. Fallani, M. Fattori, C. Fort, M. Zaccanti, G. Modugno, M. Modugno, and M. Inguscio, Anderson localization of a non-interacting Bose–Einstein condensate, *Nature*. **453**, 895 (2008).
58. J. Billy, V. Josse, Z. Zuo, A. Bernard, B. Hambrecht, P. Lugan, D. Clément, L. Sanchez-Palencia, P. Bouyer, and A. Aspect, Direct observation of Anderson localization of matter waves in a controlled disorder, *Nature*. **453**, 891 (2008).
59. A. A. Burkov, M. D. Lukin, and E. Demler, Decoherence dynamics in low-dimensional cold atom interferometers, *Phys. Rev. Lett.* **98**, 200404 (2007).